

NUCLEATION AND GROWTH OF THE SECOND STAGE CRYSTALLIZATION IN $\text{Al}_{83}\text{Ni}_{10}\text{Ce}_7$ GLASS

G.M Wang, S. H. Wang

Hebei University of Engineering, Handan China, 056038.

Introduction

Al-based amorphous alloys have been much studied in recent years because of the possibility of developing light alloys showing high strength with ductility or toughness. (1) A large number of studies have been reported that examine the first stage crystallization, when pure Al crystals form in the glass, which is identified as a growth reaction based on the quenched-in nuclei (2,3,4), while the second stage crystallization has been less studied (5). Some recent works have proved that second phase of crystallization grow rapidly with formation of a crystal-glass eutectic-like mixture, after Al stops growing in a primary crystallization(6). However, to the author knowledge, no effort has connected the crystallization mechanism of the second stage crystallization, especially for a eutectic crystallization.

In this work, we present experimental evidence of a nuclei growth reaction in the second stage crystallization for an $\text{Al}_{83}\text{Ni}_{10}\text{Ce}_7$ glass, representative of a eutectic crystallization, by means of TEM and DSC measurements. Some nuclei of the second stage precipitated phases have been identified after the first stage crystallization, followed by a slow growth reaction in the further annealing condition.

Experimental

An ingot with composition of $\text{Al}_{83}\text{Ni}_{10}\text{Ce}_7$ (at. %) was prepared by arc melting of high purity elemental metals in a pure argon atmosphere. Amorphous ribbons of thickness about 30 μm and width about 2 mm were prepared by a single roller melting-spinning apparatus at a wheel speed of 40 m/s. Differential scanning calorimetry (DSC) measurements were performed in a purified argon atmosphere using a NETZSCH - TA4. The microstructure was characterized by using a transmission electron microscopy (TEM) and a high-resolution transmission electron microscopy (HRTEM) (TECNAL 20U-TWIN.).

Result and discussion

A typical DSC curve obtained upon heating the as-quenched $\text{Al}_{83}\text{Ni}_{10}\text{Ce}_7$ sample at a rate of 20 K/min. According to the DSC scan, three temperature regions are separated in the vicinity of T_g , region A, below 559 K, region B, 559-581 K (T_x) and region C, upwards of 581 K, shown in Fig. 1 (a). Experimental methods for

observing the effect of annealing temperatures on the second stage crystallization have been illustrated in Fig. 1 (b).

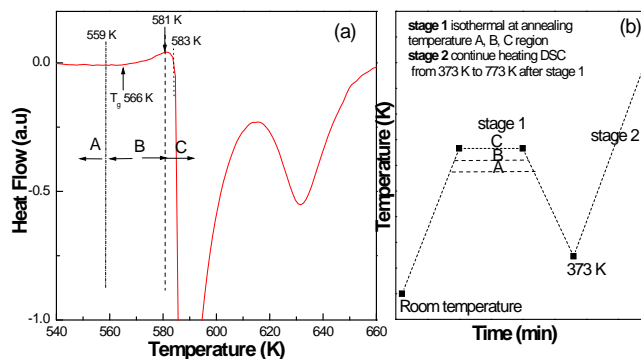


Fig.1 DSC scan (a) of $\text{Al}_{83}\text{Ni}_{10}\text{Ce}_7$ metallic glass at a rate of 20 K/min

The $\text{Al}_{83}\text{Ni}_{10}\text{Ce}_7$ samples are isothermal at temperatures from 473 to 583 K in stage 1 for 20 min, and then followed by isochronal DSC scans in stage 2, presented in Fig.2. Considering Fig.2, three characteristics are observed. At first, two exothermic peaks are observed (denoted by curve a, b and c) with the annealing temperature in region A (below 559 K) in stage 1. The higher the annealing temperature is, the weaker the second peak is. Secondly, when the annealing temperature is in region B (559-576 K) in stage 1, only one exothermic peak is observed (denoted by curve d, e and f) in stage 2. Thirdly, when the annealing temperature is in region C, no exothermic peak is observed in stage 2. These results suggest that annealing at different temperature region has different effect on the subsequent crystallization. Annealing at temperature region A affects the details of the second stage crystallization, approved by the shape change of the second exothermic peak according to the DSC curve. The matrix still keeps the amorphous characteristic, approved by the X-ray diffraction pattern (not shown) Annealing at temperature region B induces the first stage crystallization, while, annealing at temperature region C leads to a complete crystallization.

Fig. 3 shows the results of the $\text{Al}_{83}\text{Ni}_{10}\text{Ce}_7$ sample in HRTEM observations in as quenched [Fig. 3 (a)] state and TEM observations occurring on annealing temperature at 559 K for 5 min [Fig. 3 (b), (c) and (d)] and for 40 min [Fig. 3 (e)]. The as-quenched state is confirmed to be fully amorphous, without any quenched-in nuclei described in other work [9], by the broad ring diffraction pattern in Fig. 3 (a).

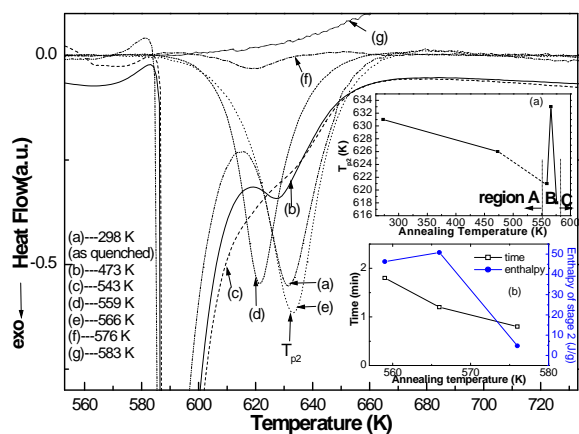


Fig. 2 DSC scans for $\text{Al}_{83}\text{Ni}_{10}\text{Ce}_7$ metallic glass in stage 2 after isothermal annealing

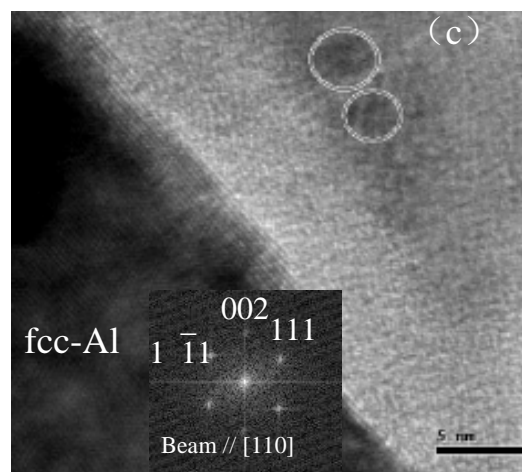
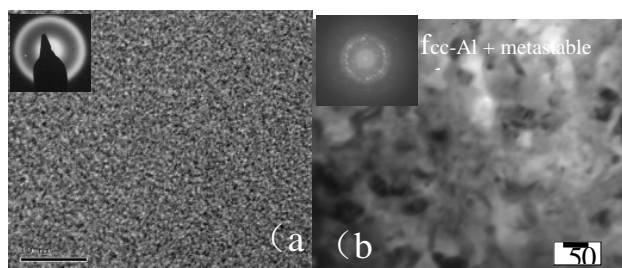


Fig.3 HRTEM image (a) of the as-quenched $\text{Al}_{83}\text{Ni}_{10}\text{Ce}_7$ glass; TEM bright-field image (b) and HRTEM images (c)

Annealing at 559 K for 5 min leads to the appearance of fcc-Al and intermetallic compounds Al_4Ce , identified by the diffraction pattern. Fcc-Al (characteristic of white particle) and Al_4Ce (the fields surrounded by the white circle) emerge in the matrix, shown in Fig. 3 (b). On some occasions, a larger number of Al nanocrystals with an average size of 6-10 nm have been well defined in Fig. 3 (c). Meanwhile, some small regions of crystal order, surrounded by black circle, randomly distribute in the fcc-Al boundary. These small regions can be attributed to the nuclei for the second stage crystallization. The appearance of Al_4Ce , fcc-Al and some nuclei is shown in Fig. 3 (d). Further annealing at 559 K for 40 min leads to a major change in microstructure, as seen in Fig. 3 (e). Al_4Ce and Al_3Ce about 1-2 μm in size, identified by the diffraction, appear in the matrix. The appearance of Al_3Ce can be attributed to the nuclei in Fig. 3 (c), which grow up to grains in the further annealing process. So, it is evidently to conclude that the nuclei of the second stage crystallization form in the first stage crystallization. Here, we suggest that the precipitation of Al and intermetallic compound, i.e. Al_4Ce is accompanied by a reconstruction of the remaining amorphous matrix in the first stage crystallization. The vacancies induced by the atom precipitating are replenished by the neighboring atoms by atomic diffusion. Therefore, it is conformable to fashion a new local solute concentration fluctuations, which are supposed to severe as the nuclei of further precipitation.



Conclusion

(i) Three temperature regions are separated in the vicinity of T_g according to the DSC scan as follow: region A, below 559 K, region B, 559 - 581 K and region C, upward of 581 K. Annealing at different region have different effect on the subsequent crystallization. For annealing at region A, the matrix still keeps the amorphous characteristics, but the second exothermic peak decay with increasing annealing temperature, inflected by the DSC scans. Annealing at region B induces the first stage crystallization, and the peak temperature and released enthalpy of the second exothermic peak has an abnormal change at T_g , as compared with annealing at other temperatures. Annealing at region C leads to a completely crystallization.

(ii) The second stage crystallization is identified as a growth reaction. The nuclei of the second stage precipitations form in the first stage crystallization. During further annealing at 559 K, growth reaction based on these nuclei leads to completely crystallization with a slow rate.

References

1. Inoue A. Prog Mater Sci 1998; 43: 345.
2. Foley JC, Allen DR and Perepezko JH. Scr. Mater 1996; 35: 555.
3. Allen D R, Foley JC and Perepezko JH. Acta Mater 1998; 46: 431.
4. Tsai AP, Kamiyama T, Kawamura Y, Inoue A and Masumoto T. Acta Mater 1997;45:1477.
5. Bassim N, Kiminami CS, Kaufman MJ. J Non-cryst Solids 2000; 271: 273.
6. Munoz-Morris MA, Surrinach S, Gich M, Baro MD and Morris DG. Acta Mater 2003; 51:1067.